

Unravelling $t\bar{t}h$ via the matrix element method

Pierre Artoisenet^a, Priscila de Aquino^b, Fabio Maltoni^c, Olivier Mattelaer^{c,d}

^a *Nikhef Theory Group, Science Park 105, 1098 XG Amsterdam, The Netherlands*

^b *Theoretische Natuurkunde and IIHE/ELEM, Vrije Universiteit Brussel, and International Solvay Institutes, Pleinlaan 2, B-1050 Brussels, Belgium*

^c *Centre for Cosmology, Particle Physics and Phenomenology (CP3),*

Université catholique de Louvain, Chemin du Cyclotron 2, B-1348 Louvain-la-Neuve, Belgium

^d *Department of Physics, University of Illinois at Urbana-Champaign, 1110 West Green Street, Urbana, IL 61801*

(Dated: January 16, 2018)

Associated production of the Higgs boson with a top-antitop pair is a key channel to gather further information on the nature of the newly discovered boson at the LHC. Experimentally, however, its observation is very challenging due to the combination of small rates, difficult multi-jet final states and overwhelming backgrounds. In the Standard Model the largest number of events is expected when $h \rightarrow b\bar{b}$, giving rise to a $W^+W^-b\bar{b}b\bar{b}$ signature, deluged in $t\bar{t}$ +jets. A promising strategy to improve the sensitivity is to maximally exploit the theoretical information on the signal and background processes by means of the matrix element method. We show how, despite the complexity of the final state, the method can be efficiently applied to discriminate the signal against combinatorial and $t\bar{t}$ +jets backgrounds. Remarkably, we find that a moderate integrated luminosity in the next LHC run will be enough to make the signature involving both W 's decaying leptonically as sensitive as the single-lepton one.

I. INTRODUCTION

Evidence for the recently discovered new heavy boson to be the long-sought-for Higgs particle of the Standard Model is already quite compelling [1, 2]. Rates and distributions are compatible with the predictions of a scalar particle coupling to other SM particles with a strength proportional to their mass. The current sensitivities and accuracies of the golden production-decay modes, however, are not sufficient to draw a final answer on the strength and the structure of the couplings without additional hypotheses. Other channels need to be investigated.

Prominent among the yet-to-be-explored production modes is the $t\bar{t}h$ associated production. The main interest of this channel stems from the fact that the rate is manifestly proportional to the square of the SM Yukawa coupling to the top quarks. In addition, more differential observables could bring information on the coupling structure [3] and on the Higgs parity [4]. This channel, however, is notoriously difficult for several reasons. The first is that production rates at hadron colliders are quite small due to the need of a large cms collision energy for the initial partons, strongly suppressed by parton distribution functions. Next-to-leading order calculations [4–7] predict a SM rate of 0.137 pb and 0.632 pb with $O(10\%)$ uncertainty at the LHC for $\sqrt{s} = 8$ and 14 TeV, respectively. Current searches mainly focus on the dominant decay mode $h \rightarrow b\bar{b}$ and therefore on a $W^+W^-b\bar{b}b\bar{b}$ final state, other decays, such as $h \rightarrow W^+W^-$ [8], $h \rightarrow \tau^+\tau^-$ [9] and eventually, $h \rightarrow \gamma\gamma$ [10], being much rarer demand larger integrated luminosities. The second reason is that the $W^+W^-b\bar{b}b\bar{b}$ signature is affected by two different types of challenging backgrounds. On the one hand $t\bar{t}$ + light- or heavy-flavor jets because of the enormous rates, and on the other hand

the intrinsic combinatorial background that stems from the difficulty of correctly identifying out of four b -jets the two from the Higgs decay. Finally, the complexity of the final state makes its kinematic reconstruction not straightforward mainly due to finite jet energy resolution, missing energy and the ubiquity of extra QCD radiation.

Due to the above intrinsic difficulties, the prospects of first using this channel for discovery or just for observation have been constantly deteriorating as more accurate predictions and simulations were available to the LHC community. More recently, the attention on this channel was revived by Plehn et al. [11] who suggested that while drastically lowering the rates, boosted tops and Higgs in the final state would make the combinatorial background much less severe, improving the significance S/\sqrt{B} of the SM Higgs observation at large enough luminosities.

In this work we argue that the sensitivity to $t\bar{t}h$ can be also enhanced at low p_T , *i.e.*, where the bulk of the cross section resides, by means of the matrix element reweighting method, improving the prospects for observation of this channel at the LHC in the coming years. The matrix element method is able to efficiently reduce the combinatorial problem for the single-lepton final states and even more for the di-lepton final state, bringing the two to a comparable level of sensitivity already for moderate integrated luminosities.

II. THE MATRIX ELEMENT METHOD

The matrix element reweighting method (MEM), originally introduced in Ref. [12], assigns probabilities to competing hypotheses, *e.g.*, signal vs. signal+background, given a sample of experimental events. The most attracting feature of this method is that it makes maximal use of both experimental information and the theoretical

model, associating a weight to each event based on the value of the matrix element (*i.e.*, the scattering amplitude) for that specific final state configuration for each of the hypotheses. While very simple in its essence, in practice several technical and conceptual challenges arise and different level of simplifications are commonly employed. The method, implemented using matrix elements calculated at the leading order, has been successfully applied to a number of key results in collider physics: from the most precise top mass determination [13, 14], single top observation [15, 16] at the Tevatron, to the Higgs boson discovery and characterization at the LHC [17, 18]. Efforts to include next-to-leading QCD corrections, at least for simple final states, have started [19, 20].

In this work, we define the weight associated with an experimental event \mathbf{x} given a set of hypotheses α as

$$P(\mathbf{x}|\alpha) = \frac{1}{\sigma_\alpha} \int d\Phi(\mathbf{y}) |M_\alpha|^2(\mathbf{y}) W(\mathbf{x}, \mathbf{y}), \quad (1)$$

where $|M_\alpha|^2(\mathbf{y})$ is the leading-order matrix element (giving the parton-level probability), $d\Phi(\mathbf{y})$ is the phase-space measure, (including the parton distribution functions $f_1(q_1)dq_1$ and $f_2(q_2)dq_2$) and $W(\mathbf{x}, \mathbf{y})$ is the transfer function which describes the evolution of (the final state) parton-level configuration in \mathbf{y} into a reconstructed event \mathbf{x} in the detector. The normalization by the total cross section σ_α in Eq. (1) ensures that $P(\mathbf{x}|\alpha)$ is a probability density, $\int P(\mathbf{x}|\alpha)d\mathbf{x} = 1$, if the transfer function is normalized to one.

As evident from the definition in Eq. (1), the calculation of each weight involves a non trivial multi-dimensional integration of complicated functions over the phase space. The problem of computing the weights for arbitrary models and processes was tackled in Ref. [21] by implementing a general algorithm in a specifically designed code named MADWEIGHT. We stress that very fact of automatically, reliably and quickly calculating weights for challenging final states as those involved in $t\bar{t}h$ has never been achieved before. It is a significant technical result on its own that provides key evidence on the generality and flexibility of the MADWEIGHT approach.

One of the main limitations of the method is that the matrix elements are considered at the leading order only and therefore extra QCD radiation effects must be handled in some effective way. In our study we are inclusive on extra transverse radiation and consider only the hardest jets to be matched with the corresponding partons in the matrix element. The transverse momentum of these partons (including isolated leptons) is assumed to be balanced against the transverse momentum of extra radiation in the event [22].

III. TECHNICAL ASPECTS

Parton-level events for signal and backgrounds are generated with MADGRAPH 5 [23], passed to PYTHIA 6 [24]

process	incl. σ	efficiency	σ^{rec}
$t\bar{t}h$, single-lepton	111 fb	0.0485	5.37 fb
$t\bar{t}h$, di-lepton	17.7 fb	0.0359	0.634 fb
$t\bar{t}$ +jets, single-lepton	256 pb	0.463×10^{-3}	119 fb
$t\bar{t}$ +jets, di-lepton	40.9 pb	0.168×10^{-3}	6.89 fb

TABLE I: Total cross sections at the LHC 14 TeV and corresponding efficiency factors of the applied selection.

for showering and hadronization, employing the MLM- k_T merging procedure [25]. Detector response simulation is performed using DELPHES 2 [26], with the input parameters tuned to the values associated with the CMS detector. Pile-up effects have not been considered.

Only the dominant background $t\bar{t}$ +jets is taken into account, and is modeled by generating parton-level $t\bar{t}$ processes with up to two extra partons in the 5-flavor scheme. For the signal, the parton-level processes $t\bar{t}h$ and $t\bar{t}h + 1$ parton are considered. Inclusive samples for the signal and the background have been normalized to the total cross section at NLO from [4] and [27], respectively. Spin correlation effects in the decays of the tops, which for signal shapes are more important than NLO QCD corrections [28], have been retained.

The event selection procedure is modeled after that adopted by the CMS collaboration for the measurement of the $t\bar{t}$ cross section in the di-lepton channel [29]. Single-lepton (di-lepton) events are required to have at least one (one pair of opposite-charge) lepton(s). Only isolated electrons or muons are lepton candidates in our analysis. They are required to have a transverse momentum $p_T > 20$ GeV and a pseudo-rapidity $|\eta| < 2.4$.

Jets are reconstructed via the anti- k_T algorithm (with a cone radius $R = 0.5$) as implemented in FASTJET [30] and applied on the calorimeter cells fired by the generated stable or quasi-stable particles. Jet candidates are required to have $p_T > 30$ GeV and $|\eta| < 2.5$, and not to overlap with any selected leptons. At least four b -jets are required. They are identified with an efficiency $\epsilon_b = 0.7$ while mis-tag rates $\epsilon_c = 0.2$ for charm quarks and $\epsilon_j = 0.015$ for light partons are used. The cross sections for signal and backgrounds together with the final efficiencies of the adopted minimal selection procedure are collected in Table I.

Only transfer functions for the jet energies are taken with a finite resolution, which we parametrize through a double-Gaussian shape function characterized by five independent parameters. For each of them, an energy dependence $c_1 + c_2\sqrt{E} + c_3E$ is used. The constants c_i are determined from an independent $t\bar{t}$ sample where well separated jets (including light and b -jets) are matched to the corresponding partons. The typical resolution for the jet energy is between 5 and 12 GeV, with tails parametrized by Gaussians of width as large as 30 GeV.

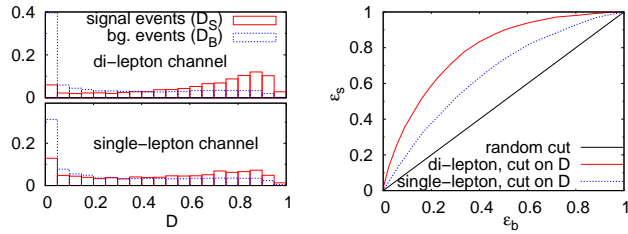


FIG. 1: Left: Normalized distributions of events with respect to the MEM-based observable D for the di-lepton (top) and single-lepton (bottom) channels. Right: Efficiency of selecting signal vs. background using a $D > D_{min}$ cut.

IV. RESULTS

For a generic event i with kinematics \mathbf{x}_i the MEM-based observable D_i is defined as follows:

$$D_i = \frac{P(\mathbf{x}_i|S)}{P(\mathbf{x}_i|S) + P(\mathbf{x}_i|B)}. \quad (2)$$

Expected (normalized) distributions of signal and background events with respect to this observable are named D_S and D_B , and are shown in Fig. 1 (left). The plots show that for the same number of signal events the MEM-based observable delivers a higher discriminating power in the case of the di-lepton channel. This is manifest in the right-hand plot of the same figure where the ϵ_s versus ϵ_b efficiencies resulting from a cut on the observable $D > D_{min}$ are shown. This may seem surprising at first sight, given that the di-lepton channel is characterized by two missing particles in the final state, against only one in the single-lepton channel. However, the di-lepton channel is much cleaner, with only b -jets required in the final state, a lower probability of erroneously including extra QCD radiation and, eventually, a more manageable combinatorial background.

In order to assess the significance that can be achieved at the LHC $\sqrt{s} = 14$ TeV for a given luminosity \mathcal{L} , we consider a large number of pseudo-experiments, each with a number of events set to $N = \sigma_{bg}^{rec} \mathcal{L}$ (with σ_{bg}^{rec} the reconstructed cross section, see Table I, last column). In the B -only hypothesis, the number of signal and background events are set to $s = 0$ and $b = N$. In the $S + B$ hypothesis, s and b are generated under the constraint $s + b = N$ according to the product of Poisson distributions with mean values $Ns_0/(s_0 + b_0)$ and $Nb_0/(s_0 + b_0)$, respectively. Here s_0 and b_0 are the expected number of reconstructed events after rescaling the signal cross section by a parameter μ , *i.e.* $b_0 = \sigma_{bg}^{rec} \mathcal{L}$ and $s_0 = \mu \sigma_{sig}^{rec} \mathcal{L}$. For each event, the corresponding D_i value is generated according to the probability law D_S (in the case of a signal event) or D_B (in the case of a background event) shown in Fig. 1. This procedure is used to generate 10^4 pseudo-experiments under each hypothesis (B -only or $S+B$) at a given luminosity \mathcal{L} .

For each pseudo-experiment the likelihood ratio L^R is

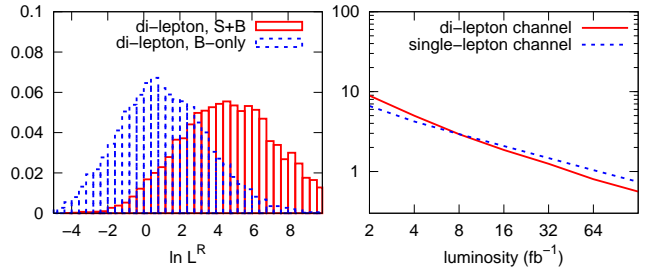


FIG. 2: Left: Log likelihood profiles in the case of the di-lepton channel, assuming a luminosity of 32 fb^{-1} at 14 TeV and setting $\mu = 1$ (SM cross section). Right: Expected upper bound on the $t\bar{t}h$ cross section (in units of SM cross section) based on 95 % C.L.

calculated as follows:

$$\begin{aligned} L^R &= \prod_i^N \frac{r_0 P(\mathbf{x}_i|S) + (1 - r_0) P(\mathbf{x}_i|B)}{P(\mathbf{x}_i|B)} \\ &= \prod_i^N \frac{r_0 D_i + (1 - r_0)(1 - D_i)}{(1 - D_i)}, \end{aligned} \quad (3)$$

with $r_0 = s_0/(s_0 + b_0)$. The resulting B -only and $S + B$ distributions of pseudo-experiments with respect to $\ln(L^R)$ are shown in Fig. 2 (left) in the case of the di-lepton channel, with $\mathcal{L} = 32 \text{ fb}^{-1}$ and $\mu = 1$. The two distributions are shifted towards positive values of $\ln(L^R)$, which indicates that the MEM weights do not exactly describe the phase-space distributions of background and signal events. This bias originates from the approximations inherent to the calculation of the weights, *e.g.*, the assumed parametrization of the transfer function and the effective treatment of beyond-leading-order QCD radiations.

By smearing the value of b_0 according to a log-normal distribution (mean= b_0 , std= $0.2b_0$) before generating s and b in each pseudo-experiment, we also verified that systematic uncertainties on the background normalization have a negligible impact on the distributions of pseudo-experiments with respect to $\ln(L^R)$. On the other hand, already a 20% uncertainty on b_0 hampers a counting analysis based on the number of events to be available at LHC, unless $s/b \gg 0.2$.

We repeat this exercise with different values of μ until the median of the B -only distribution cuts 5% of the left-hand tail of the $S + B$ distribution. Such a value of μ provides us with the estimate $\mu \times \sigma(t\bar{t}h)$ of the expected upper bound on the signal cross section at 95 % C.L. in the absence of signal. Fig. 2 (right) shows our estimate of the parameter μ as a function of the luminosity \mathcal{L} , separately for the di-lepton and single-lepton channels. We observe that the sensitivity achieved in the di-lepton channel is slightly better than the one in the single-lepton channel at large luminosities.

V. CONCLUSIONS

The matrix element reweighting method is a powerful technique to enhance the sensitivity of searches and measurements at colliders. In this work we have applied it to the observation of Higgs production in association with $t\bar{t}$ pair, in particular to final state signatures involving the decay of the Higgs to bottom quarks. First, we have verified that the general algorithm implemented in MADWEIGHT provides the possibility of automatically, reliably and quickly calculating weights for final states as complex as those featured in $t\bar{t}h$. This technical result, by itself, is an important one as it opens the door to applications of the MEM to a much wider set of processes and analyses than what has been done so far. Second, we have applied the method to $t\bar{t}h$ with both one- and two-lepton final states. We have found that the dilepton final state, though penalized by a smaller number of expected events and possibly more difficult to reconstruct due to the presence of two neutrinos in the final state, becomes competitive with the single-lepton channel already after a moderate integrated luminosity. We reckon that this result, while based on MC simulations, is rather robust and encourage more refined investigations. For instance, relaxing the number of requested b -tags to three in the di-lepton final state would bring a significant increase in the statistics, yet not of the combinatorial background, leading to a further relative gain with respect to the single-lepton final state. Analogously, the inclusion of pile-up will impact more the signature with

the largest number of jets in the final state. Only fully-fledged experimental analyses can assess the final gains, and correctly include the systematic uncertainties that have been neglected here.

In conclusion the search for SM $t\bar{t}h$ and in particular the di-lepton final state is a perfect illustration of the power of the matrix element method in providing additional leverage in difficult analyses. Further investigations concerning the possibility of using the matrix element method in $t\bar{t}h$ to access more detailed information on the structure of the couplings of the new boson or in other very challenging production channels, such as thj [31], are foreseen.

VI. ACKNOWLEDGEMENTS

We are grateful to J. D' Hondt, K. Cranmer, R. Frederix, and to many CP3 members for very useful information exchange and discussions. P.A. is supported by a Marie Curie Intra-European Fellowship (PIEF-GA-2011-299999 PROBE4TeVSCALE). P.d.A. is supported in part by the Belgian Federal Science Policy Office through the Interuniversity Attraction Pole P7/37, in part by the "FWO-Vlaanderen" through the project G.0114.10N, and in part by the Concerted Research action "Supersymmetric Models and their Signatures at the Large Hadron Collider" of the Vrije Universiteit Brussel (VUB)". O.M. is fellow of the Belgian American Education Foundation.

-
- [1] CMS-HIG-13-003. CMS-HIG-13-004. CMS-HIG-13-006. CMS-HIG-13-009. (2013).
 - [2] ATLAS-CONF-2013-009. ATLAS-CONF-2013-010. ATLAS-CONF-2013-012. ATLAS-CONF-2013-013. (2013).
 - [3] C. Degrande, J. Gerard, C. Grojean, F. Maltoni, and G. Servant, *JHEP* **1207**, 036 (2012), 1205.1065.
 - [4] R. Frederix, S. Frixione, V. Hirschi, F. Maltoni, R. Pittau, and P. Torrielli, *Phys.Lett.* **B701**, 427 (2011), 1104.5613.
 - [5] W. Beenakker, S. Dittmaier, M. Kramer, B. Plumper, M. Spira, et al., *Phys.Rev.Lett.* **87**, 201805 (2001), hep-ph/0107081.
 - [6] S. Dawson, L. Orr, L. Reina, and D. Wackerroth, *Phys.Rev.* **D67**, 071503 (2003), hep-ph/0211438.
 - [7] M. Garzelli, A. Kardos, C. Papadopoulos, and Z. Trocsanyi, *Europhys.Lett.* **96**, 11001 (2011), 1108.0387.
 - [8] F. Maltoni, D. L. Rainwater, and S. Willenbrock, *Phys.Rev.* **D66**, 034022 (2002), hep-ph/0202205.
 - [9] A. Belyaev and L. Reina, *JHEP* **0208**, 041 (2002), hep-ph/0205270.
 - [10] C. Buttar, S. Dittmaier, V. Drollinger, S. Frixione, A. Nikitenko, et al. (2006), hep-ph/0604120.
 - [11] T. Plehn, G. P. Salam, and M. Spannowsky, *Phys.Rev.Lett.* **104**, 111801 (2010), 0910.5472.
 - [12] K. Kondo, *J.Phys.Soc.Jap.* **57**, 4126 (1988).
 - [13] V. Abazov et al. (D0 Collaboration), *Nature* **429**, 638 (2004), hep-ex/0406031.
 - [14] A. Abulencia et al. (CDF Collaboration), *Phys.Rev.* **D75**, 031105 (2007), hep-ex/0612060.
 - [15] T. Aaltonen et al. (CDF Collaboration), *Phys.Rev.Lett.* **103**, 092002 (2009), 0903.0885.
 - [16] V. Abazov et al. (D0 Collaboration), *Phys.Rev.Lett.* **103**, 092001 (2009), 0903.0850.
 - [17] G. Aad et al. (ATLAS Collaboration), *Phys.Lett.* **B716**, 1 (2012), 1207.7214.
 - [18] S. Chatrchyan et al. (CMS Collaboration), *Phys.Lett.* **B716**, 30 (2012), 1207.7235.
 - [19] J. M. Campbell, W. T. Giele, and C. Williams, *JHEP* **1211**, 043 (2012), 1204.4424.
 - [20] J. M. Campbell, R. K. Ellis, W. T. Giele, and C. Williams (2013), 1301.7086.
 - [21] P. Artoisenet, V. Lemaître, F. Maltoni, and O. Mattelaer, *JHEP* **1012**, 068 (2010), 1007.3300.
 - [22] J. Alwall, A. Freitas, and O. Mattelaer, *Phys.Rev.* **D83**, 074010 (2011), 1010.2263.
 - [23] J. Alwall, M. Herquet, F. Maltoni, O. Mattelaer, and T. Stelzer, *JHEP* **1106**, 128 (2011), 1106.0522.
 - [24] T. Sjostrand, S. Mrenna, and P. Z. Skands, *JHEP* **0605**, 026 (2006), hep-ph/0603175.
 - [25] J. Alwall, S. de Visscher, and F. Maltoni, *JHEP* **0902**, 017 (2009), 0810.5350.

- [26] S. Oryn, X. Rouby, and V. Lemaître (2009), 0903.2225.
- [27] M. Cacciari, M. Czakon, M. Mangano, A. Mitov, and P. Nason, *Phys.Lett.* **B710**, 612 (2012), 1111.5869.
- [28] P. Artoisenet, R. Frederix, O. Mattelaer, and R. Rietkerk (2012), 1212.3460.
- [29] S. Chatrchyan et al. (CMS Collaboration) (2012), 1211.2220.
- [30] M. Cacciari, G. P. Salam, and G. Soyez, *Eur.Phys.J.* **C72**, 1896 (2012), 1111.6097.
- [31] M. Farina, C. Grojean, F. Maltoni, E. Salvioni, and A. Thamm (2012), 1211.3736.